

# Achieving low sub-0.6-nm EOT in gate-first *n*-MOSFET with TiLaO/CeO<sub>2</sub> gate stack

C.H. Cheng<sup>a,\*</sup>, K.I. Chou<sup>b</sup>, Albert Chin<sup>b</sup>

<sup>a</sup> Department of Mechatronic Technology, National Taiwan Normal University, Taipei 106, Taiwan

<sup>b</sup> Department of Electronics Engineering, National Chiao Tung University, Hsinchu 300, Taiwan

## ARTICLE INFO

### Article history:

Received 22 November 2012

Received in revised form 26 January 2013

Accepted 10 February 2013

The review of this paper was arranged by Prof. S. Cristoloveanu

### Keywords:

Gate first

TiLaO

CeO<sub>2</sub>

Small EOT

## ABSTRACT

We report a gate-first TiLaO/CeO<sub>2</sub> *n*-MOSFET with an equivalent oxide thickness (EOT) of only 0.56 nm and threshold voltage ( $V_t$ ) of 0.31 V. This small EOT MOSFET was achieved by employing high- $\kappa$  CeO<sub>2</sub> interfacial layer with high bond enthalpy (795 kJ/mol) to replace low- $\kappa$  SiO<sub>2</sub> with close bond enthalpy (800 kJ/mol). The cerium silicate can aggressively scale EOT down to sub-0.6-nm EOT region without increasing gate leakage, which is urgently needed for 16 nm technology node.

© 2013 Elsevier Ltd. All rights reserved.

## 1. Introduction

Recently, a major challenge for metal-gate/high- $\kappa$  CMOS [1–13] is to trade off equivalent oxide thickness (EOT) and flat-band voltage ( $V_{fb}$ ) roll-off at a CMOS-compatible gate first process, since the large  $V_{fb}$  roll-off [7,8] at smaller equivalent oxide thickness (EOT) is undesirable, which can result in an unwanted high threshold voltage ( $V_t$ ). Previously we have shown that the  $V_{fb}$  roll-off and the high  $V_t$  are related to charged-oxygen vacancies in the non-stoichiometric oxides (HfO<sub>2-x</sub> and SiO<sub>x</sub>) [7,8]. The vacancy-rich interfacial layer not only leads to  $V_{fb}$  roll-off and high  $V_t$ , but also largely increase gate leakage current at a sub-nm EOT region. Although an ultra-thin SiO<sub>2</sub> layer can be used as interface layer between high- $\kappa$  dielectric and Si to reach a 1 nm EOT [9] in the 45 nm node technology, this may not work as the gate-stack technology is highly scaled down to sub-0.6-nm EOT for 16 nm technology node. To solve these issues, we proposed a stacked gate dielectric using higher- $\kappa$  TiLaO [14] and large-bandgap cerium oxide (CeO<sub>2</sub>) interface layer with bond enthalpy (795 kJ/mol) close to that of the SiO<sub>2</sub> (800 kJ/mol) [3] for aggressive EOT scaling. Since the TiO<sub>2</sub>-based dielectrics in direct contact with Si substrate always accompany common shortcoming of poor interface quality, the robust cerium-based silicate to improve the interface thermal stability become more urgent.

In this paper, TiLaO/CeO<sub>2</sub> *n*-MOSFET using silicate interface modification to obtain a small 0.56 nm EOT and a low  $V_t$  of 0.31 V have been demonstrated. The *n*-MOSFET with highly scaled EOT can be attributed to the combined results of an increased capacitance density using higher- $\kappa$  TiLaO gate dielectric, low gate leakage and robust cerium-based silicate interface.

## 2. Experimental procedure

Standard p-type Si wafers were used in this study. The simple, self-aligned, gate-first TaN/TiLaO/CeO<sub>2</sub> *n*-MOSFETs were made by depositing TiO<sub>2</sub>-doped La<sub>2</sub>O<sub>3</sub> (~25% TiO concentration) on Si substrate using electron beam (e-beam) evaporation, followed by a post-deposition anneal (PDA) of 400 °C. The low-temperature physical-vapor disposition [3–8,13,14] have less interface reaction compared to sputtering with plasma damage or high-temperature chemical-vapor disposition. The adding TiO<sub>2</sub> in TiLaO increases the dielectric constant ( $\kappa$  value), which allows using a thicker layer to decrease the gate leakage without sacrificing gate capacitance density to reach small EOT. Then 150-nm-thick TaN were subsequently deposited on these gate stacks and RTA annealed at 550–900 °C to form the MOS capacitors. For comparison, the same MOS process was also used to fabricate other TaN/TiLaO/Al<sub>2</sub>O<sub>3</sub>/p-Si *n*-MOS capacitors. After patterning, self-aligned As<sup>+</sup> implantation with an acceleration voltage of 25 KeV and a dosage of  $5 \times 10^{15}$  cm<sup>-2</sup> for source-drain doping was applied and activated at 900 °C RTA. After etching non-reacted metal, Al contact metal was added on source-drain to form the *n*-MOSFETs with 10- $\mu$ m (100- $\mu$ m size). The

\* Corresponding author.

E-mail address: [chcheng@ntnu.edu.tw](mailto:chcheng@ntnu.edu.tw) (C.H. Cheng).

interface reaction was investigated by Transmission Electron microscopy (TEM). The fabricated *n*-MOSFETs were characterized by capacitance–voltage (*C*–*V*) and current–voltage (*J*–*V*) measurements. The EOT extractions of experimental *C*–*V* curves were well fitted by CVC simulators.

### 3. Results and discussion

Fig. 1a and b shows the *C*–*V* and *J*–*V* curves of TaN/TiLaO *n*-MOS devices at various RTA temperatures. High capacitance density of  $3.3 \mu\text{F}/\text{cm}^2$ , leakage current of  $6.7 \times 10^{-2} \text{ A}/\text{cm}^2$  at  $-1 \text{ V}$  and proper  $V_{fb}$  of  $-0.6 \text{ V}$  are obtained after  $800^\circ\text{C}$  RTA. This gives an EOT of  $0.72 \text{ nm}$  by CVC Quantum-Mechanical *C*–*V* simulation. The large negative  $V_{fb}$  with thickness dependence is unique property of  $\text{La}_2\text{O}_3$  dielectric [6]. Both the increased capacitance density for a reduced EOT and negative  $V_{fb}$  shift are observed with increasing thermal budget from  $400^\circ\text{C}$  PDA to  $800^\circ\text{C}$  RTA. It is demonstrated that the gate dielectric was densified but thicker interfacial layer were also formed after  $800^\circ\text{C}$  RTA. The TEM images of MOS sample with  $800^\circ\text{C}$  RTA was inserted in Fig. 1a, where the  $1.2\text{-nm}$ -thick interfacial layer was clearly observed. Such interfacial layer formation is unavoidable because of the strong bond enthalpy of Si–O ( $800 \text{ kJ}/\text{mol}$ ) close to La–O ( $799 \text{ kJ}/\text{mol}$ ) but higher than Ti–O ( $672 \text{ kJ}/\text{mol}$ ) [3]. Furthermore, the titanium-based silicate interface with higher interface states is unstable. The severe  $V_{fb}$  roll-off to positive bias direction and degraded capacitance density were found when increasing RTA temperature up to  $900^\circ\text{C}$  (not shown here).

To prevent from  $V_{fb}$  roll-off and unstable interface formation at a gate first process, the high- $\kappa$   $\text{CeO}_2$  was used to improve interface

thermal stability of higher- $\kappa$  TiLaO dielectric. Fig. 2a and b shows the *C*–*V* and *J*–*V* curves of TiLaO/ $\text{CeO}_2$  *n*-MOS devices with different RTA conditions. The capacitance density of  $2.3 \mu\text{F}/\text{cm}^2$  and gate leakage current of  $1.1 \times 10^{-2} \text{ A}/\text{cm}^2$  at  $-1 \text{ V}$  were measured at a low  $550^\circ\text{C}$  RTA. However, a very high capacitance density of  $4.2 \mu\text{F}/\text{cm}^2$  and low leakage current of  $1.2 \text{ A}/\text{cm}^2$  at  $-1 \text{ V}$  were further reached after a high thermal budget of  $900^\circ\text{C}$ . The high-density gate capacitance provides a small EOT of  $0.56 \text{ nm}$ , which can be used for  $16 \text{ nm}$  technology node with  $10 \text{ nm}$  gate length according to ITRS. As shown in TEM image of Fig. 2c, a cerium–silicate (checked by EDX) with sharp interface was found within the  $3.6\text{-nm}$ -thick TiLaO/ $\text{CeO}_2$  gate dielectric stack, giving a high- $\kappa$  value of 25. Thus, the well-behaved *C*–*V* curves and the increased capacitance density by 82% from  $500^\circ\text{C}$  to  $900^\circ\text{C}$  RTA explain that

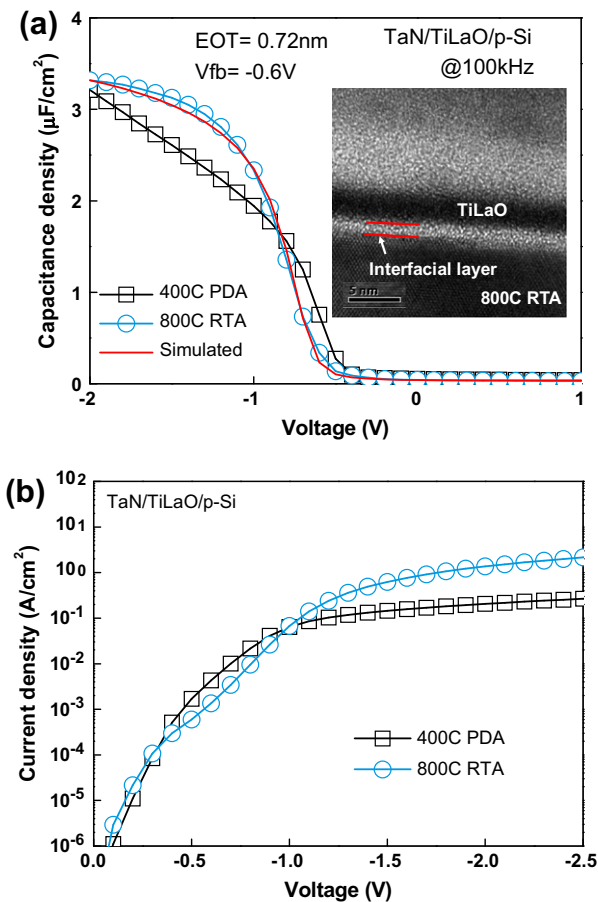


Fig. 1. (a) *C*–*V* and (b) *J*–*V* characteristics of TiLaO *n*-MOS capacitors with  $400^\circ\text{C}$  PDA and  $800^\circ\text{C}$  RTA. The inset figure is cross-sectional TEM picture of TiLaO *n*-MOS capacitors after  $800^\circ\text{C}$  RTA.

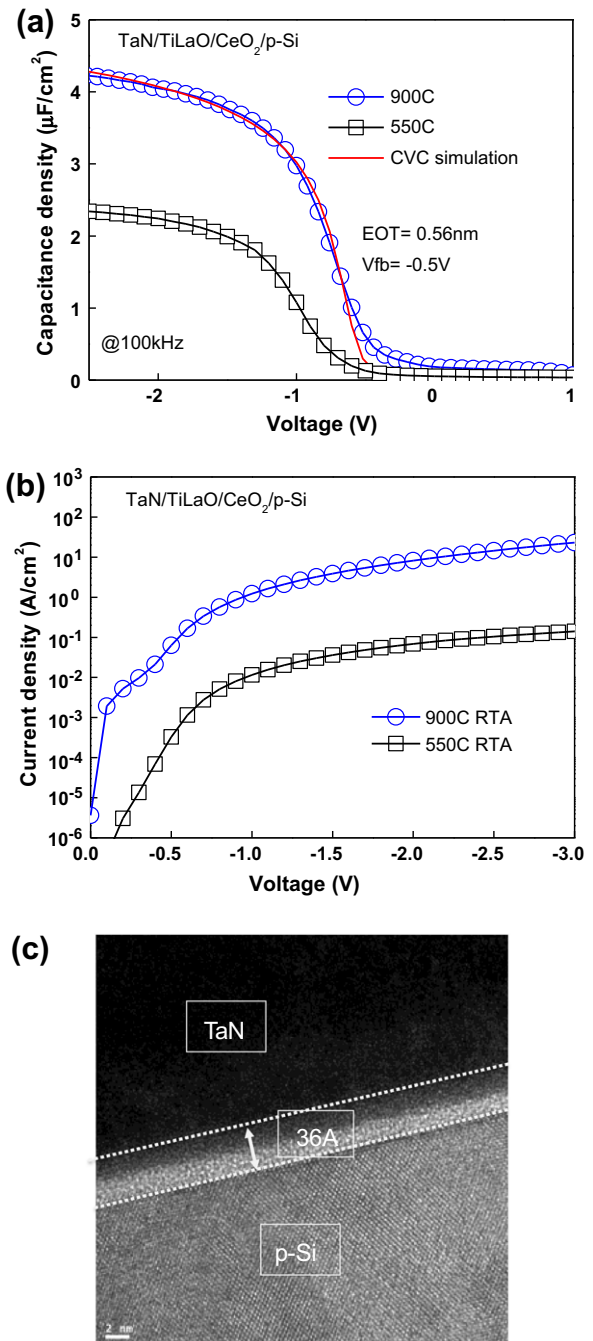


Fig. 2. (a) *C*–*V*, (b) *J*–*V* characteristics and (c) cross-sectional TEM picture of TiLaO/ $\text{CeO}_2$  *n*-MOS capacitors.

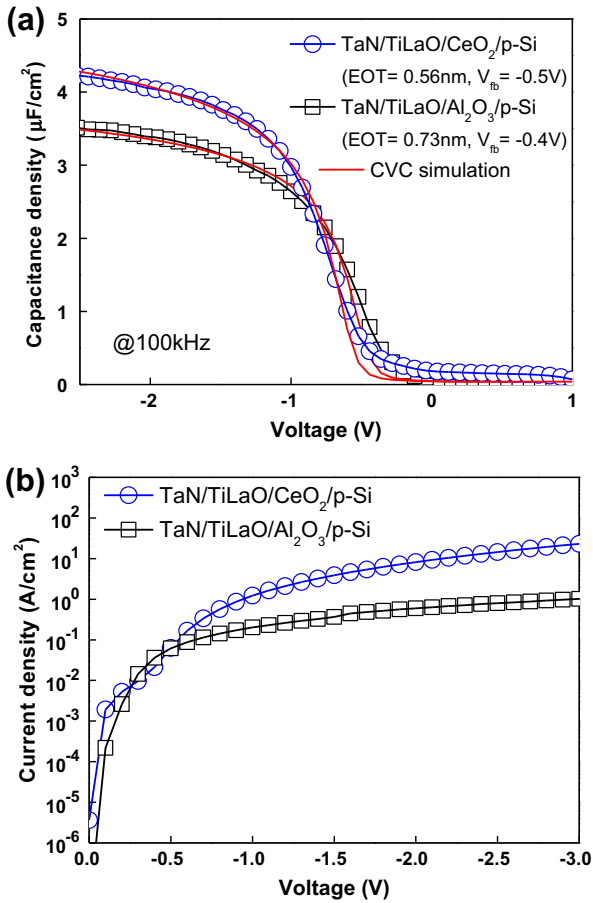


Fig. 3. (a) C–V and (b) J–V characteristics TiLaO/[CeO<sub>2</sub> or Al<sub>2</sub>O<sub>3</sub>] n-MOS capacitors.

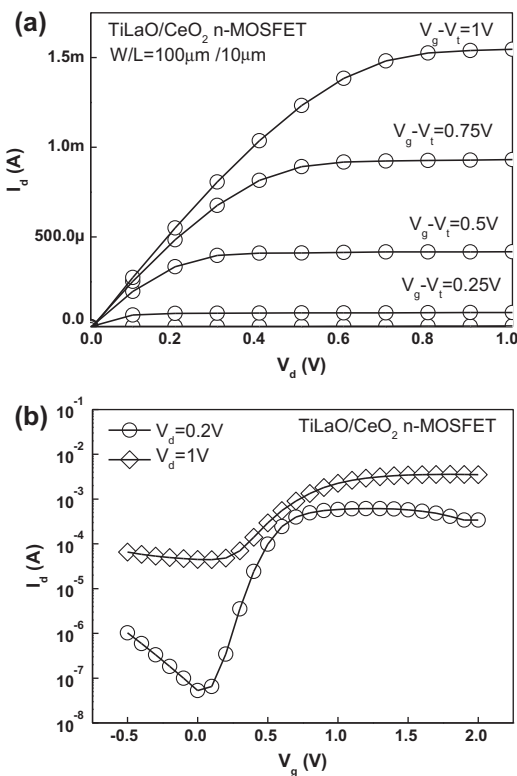


Fig. 4. (a)  $I_d$ – $V_d$  and (b)  $I_d$ – $V_g$  characteristics of TiLaO/CeO<sub>2</sub> n-MOSFETs.

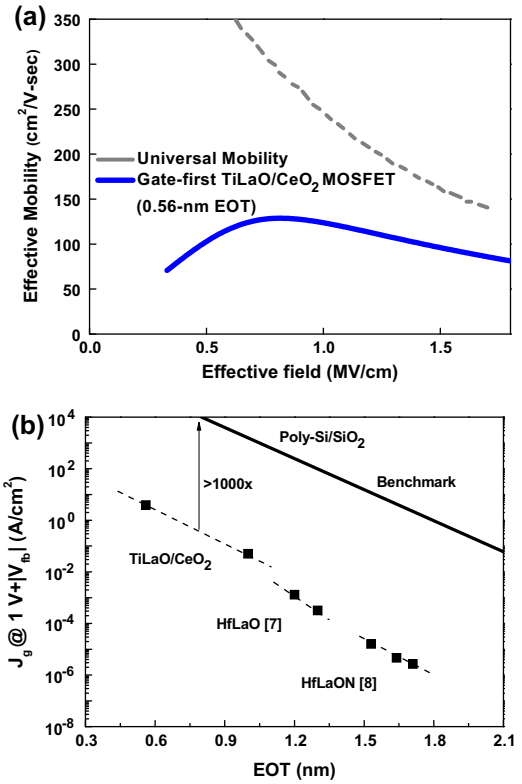


Fig. 5. (a) Electron mobility and (b) EOT verse gate leakage (EOT– $J_g$ ) characteristics of TiLaO/CeO<sub>2</sub> n-MOSFETs.

the observed interfacial layer is robust cerium silicate rather than low- $\kappa$  defective SiO<sub>2</sub>.

From the viewpoint of EOT scaling, the Al<sub>2</sub>O<sub>3</sub> dielectric with large bandgap and good thermal stability is suitable as buffered layer to resist the formation of defective interfacial layer. Thus, we also fabricated a TiLaO/Al<sub>2</sub>O<sub>3</sub> n-MOS device as a control sample for comparison. Fig. 3a and b shows the C–V and J–V curves of TaN/TiLaO/[CeO<sub>2</sub> or Al<sub>2</sub>O<sub>3</sub>] n-MOS capacitors after 900 °C RTA. Compared to TiLaO/CeO<sub>2</sub> n-MOS, TiLaO/Al<sub>2</sub>O<sub>3</sub> one has a lower capacitance density of 3.5  $\mu\text{F}/\text{cm}^2$  and larger 0.73-nm EOT, which cannot meet the requirement of sub-0.6-nm EOT at 16 nm technology node. The negative  $V_{fb}$  (–0.4 V) with slightly positive shift is believed to be related to the intrinsic dipole effect near Al-based interfacial layer that it is favorable for  $V_t$  tuning in p-MOSFET.

Fig. 4a and b shows the  $I_d$ – $V_d$  and  $I_d$ – $V_g$  characteristics of TiLaO/CeO<sub>2</sub> n-MOSFET. In addition to output transistor characteristics, the low  $V_t$  of 0.31 V was measured at this 0.56-nm-EOT transistor. Fig. 5a shows the effective mobility extracted by split CV measurement based on linear  $I_d$ – $V_g$  characteristic in TiLaO/CeO<sub>2</sub> n-MOSFETs. The universal mobility of conventional MOSFET was plotted for comparison. A mobility of 126  $\text{cm}^2/\text{V}\cdot\text{s}$  at 0.8 MV/cm was obtained in TiLaO/CeO<sub>2</sub> n-MOSFET with a 0.56 nm EOT. It has been clarified that such low  $V_t$  and EOT can be attributed to the unique negative  $V_{fb}$  of La<sub>2</sub>O<sub>3</sub> in bulk TiLaO and robust cerium silicate interface with high bond enthalpy. However, the device mobility is significantly smaller than the TiN/HfO<sub>2</sub> n-MOSFET with a 1 nm EOT [11]. The mobility degradation at small sub-0.6-nm EOT is unavoidable due to charged vacancies in the dielectric or related remote phonon scattering. Although the interface state is high at this small-EOT MOSFET with gate first process, further improvement on mobility can be expected by inserting an ultrathin oxide [15] or low-temperature junction formation by solid-phase diffusion [13]. Besides, the gate leakage at 1 V above  $V_{fb}$  for TiLaO/CeO<sub>2</sub> n-MOSFET still can maintain  $\geq 3$  orders of magnitude lower

than that of benchmark SiO<sub>2</sub> while EOT scaling from 1 nm to 0.56 nm, as shown in Fig. 5b.

#### 4. Conclusions

We report a gate-first *n*-MOSFET with a low EOT of 0.56 nm using gate stack of TiLaO/CeO<sub>2</sub>. The robust cerium silicate interfacial layer was used to prevent from additional EOT increase at a gate-first process, which enabled aggressive EOT scaling down to <0.6 nm target of 16 nm technology node. Thus, this self-aligned and gate-first *n*-MOSFET with a highly scaled EOT is compatible with CMOS process.

#### References

- [1] Tseng H-H, Capasso CC, Schaeffer JK, Hebert EA, Tobin PJ, Gilmer DC, et al. IEDM Technol Dig 2004:821–4.
- [2] Nabatame T, Kadoshima M, Iwamoto K, Mise N, Migita S, Ohno M, et al. IEDM Technol Dig 2004:83–6.
- [3] Yu DS, Chin Albert, Wu CH, Li M-F, Zhu C, Wang SJ, et al. IEDM Technol Dig 2005:649–52.
- [4] Wu CH, Yu DS, Chin Albert, Wang SJ, Li M-F, Zhu C, et al. IEEE Electron Device Lett 2006;27:90–2.
- [5] Wang XP, Shen C, Li M-F, Yu HY, Sun Y, Feng YP, et al. Symp VLSI Technol Dig 2006:12–3.
- [6] Wu CH, Hung BF, Chin Albert, Wang SJ, Wang XP, Li M-F, et al. IEDM Technol Dig 2006:617–20.
- [7] Cheng CF, Wu CH, Su NC, Wang SJ, McAlister SP, Chin Albert. IEDM Technol Dig 2007:333–6.
- [8] Liao CC, Chin Albert, Su NC, Li M-F, Wang SJ. Symp VLSI Technol Dig 2008:190–1.
- [9] Mistry K, Allen C, Auth C, Beattie B, Bergstrom D, Bost M, et al. IEDM Technol Dig 2007:247–50.
- [10] Takahashi M, Ogawa A, Hirano A, Kamimuta Y, Watanabe Y, Iwamoto K, et al. IEDM Technol Dig 2007:523–6.
- [11] Datta S, Dewey G, Doczy M, Doyle BS, Jin B, Kavalieros J, et al. IEDM Technol Dig 2003:653–6.
- [12] Tsai W, -Å Ragnarsson L, Pantisano L, Chen PJ, Onsia B, Schram T, et al. IEDM Technol Dig 2003:311–4.
- [13] Lin SH, Liu SL, Yeh FS, Chin Albert. IEEE Electron Device Lett 2009;30:75–7.
- [14] Cheng CH, Pan HC, Yang HJ, Hsiao CN, Chou CP, McAlister SP, et al. IEEE Electron Device Lett 2007;28:1095–7.
- [15] Chang MF, Lee PT, Chin Albert. IEEE Electron Device Lett 2009;30:861–3.